HHS Public Access

Author manuscript

FEBS J. Author manuscript; available in PMC 2019 July 01.

Published in final edited form as:

FEBS J. 2011 May ; 278(9): 1533–1546. doi:10.1111/j.1742-4658.2011.08077.x.

A structured RNA in hepatitis B virus post-transcriptional regulatory element represses alternative splicing in a sequence-independent and position-dependent manner

Chen Huang[1,2], **Mao-Hua Xie**[1], **Wei Liu**[1], **Bo Yang**[1], **Fan Yang**[1], **Jingang Huang**[1], **Jie Huang**[1], **Qijia Wu**[1], **Xiang-Dong Fu**[1,3], and **Yi Zhang**[1,2]

[1] State Key Laboratory of Virology, College of Life Sciences, Wuhan University, Hubei, China

[2] Center for Genome Analysis, ABLife Inc., Dong-Hu-Ming-Ju, Wuhan, Hubei, China

[3] Department of Cellular and Molecular Medicine, University of California, San Diego, La Jolla, CA, USA

Abstract

Hepatitis B virus (HBV) transcripts are subjected to multiple splicing decisions, but the mechanism of splicing regulation remains poorly understood. In this study, we used a well-investigated alternative splicing reporter to dissect splicing regulatory elements residing in the post-transcriptional regulatory element (PRE) of HBV. A strong intronic splicing silencer (ISS) with a minimal functional element of 105 nucleotides (referred to as PREISS) was identified and, interestingly, both the sense and antisense strands of the element were found to strongly suppress alternative splicing in multiple human cell lines. PRE-ISS folds into a double-hairpin structure, in which substitution mutations disrupting the double-hairpin structure abolish the splicing silencer activity. Although it harbors two previously identified binding sites for polypyrimidine tract binding protein, PRE-ISS represses splicing independent of this protein. The silencing function of PRE-ISS exhibited a strong position dependence, decreasing with the distance from affected splice sites. PRE-ISS does not belong to the intronic region of any HBV splicing variants identified thus far, preventing the testing of this intronic silencer function in the regulation of HBV splicing. These findings, together with the identification of multiple sense–antisense ISSs in the HBV genome, support the hypothesis that a sequence-independent and structure-dependent regulatory mechanism may have evolved to repress cryptic splice sites in HBV transcripts, thereby preventing their aberrant splicing during viral replication in the host.

Correspondence Y. Zhang, Center for Genome Analysis, ABLife Inc., Dong-Hu-Ming-Ju, Room, 1-2-1202, 18 North Zhuo-Dao-Quan Road, Wuhan, Hubei 430079, China, Fax: 86 27 68754945, Tel: 86 27 87153085, yizhang101@hotmail.com.

Supporting information

The following supplementary material is available:

This supplementary material can be found in the online version of this article.

Please note: As a service to our authors and readers, this journal provides supporting information supplied by the authors. Such materials are peer-reviewed and may be re-organized for online delivery, but are not copy-edited or typeset. Technical support issues arising from supporting information (other than missing files) should be addressed to the authors.

Keywords

alternative splicing; HBV PRE; hepatitis B virus (HBV); intronic splicing silencer (ISS); RNA structure

Introduction

Alternative splicing occurs in as many as 95% of human genes with multiple exons [1,2], generating multiple mRNA isoforms from the same gene transcript, which is thought to contribute to proteome complexity, tissue and physiological specificity, and functional diversity in mammalian cells [3,4]. Accurate recognition of splice sites in higher eukaryotes requires not only core splice signals, including highly degenerate 5′ and 3′ splice sites, branch point sequence and the polypyrimidine tract, but also various auxiliary splicing regulatory elements (SREs) present in exons and introns that are conventionally categorized as exonic splicing enhancers (ESEs), exonic splicing silencers (ESSs), intronic splicing enhancers (ISEs) and intronic splicing silencers (ISSs) according to their function and location in pre-mRNA [5]. In general, the majority of known *cis*-acting SREs act by recruiting *trans*-acting splicing factors that activate or repress the usage of nearby splice sites. Although not exclusively, most splicing enhancers tend to bind SR proteins, a family of proteins containing one or two RNA-binding domains and a signature RS domain rich in Arg/Ser dipeptides, and splicing silencers usually recruit heterogeneous nuclear RNPs, a set of proteins with diverse structures and functions [6]. In higher eukaryotes, multiple regulatory parameters, such as the splice site strength, the interaction between *cis*-acting SREs and the corresponding splicing factors, the RNA secondary structures, the exon/intron architecture and the process of pre-mRNA synthesis, may be elaborately integrated to achieve flexible, yet controllable, splice site selection [7].

Recently, genome-wide computational analysis has revealed that RNA secondary structure is prevalent around the functional splice sites in human genes, which may generally contribute to the regulation of alternative splicing [8]. It has been well established that RNA secondary structure interferes with the accessibility of core splicing signals by shielding the signals in the base-paired region [9,10]. Furthermore, RNA structure has been found to regulate the accessibility of auxiliary SREs to splicing factors, such as in regulated splicing of the fibronectin EDA exon [11].

RNA secondary structures have been shown to be extensively involved in the control of viral gene expression [12,13]. Recent studies have led to the appreciation of their roles in regulating the splicing of HIV-1 transcripts [14]. Hepatitis B virus (HBV) infects more than 2 billion people worldwide, causing acute and chronic hepatitis, hepatocirrhosis and hepatocellular carcinoma. The pre-genomic RNA (pgRNA) of HBV can be alternatively spliced to generate up to 13 splice variants identified in clinical samples [15], and some splicing products have been shown to modulate viral replication and persistence [16–18]. However, the mechanism of the control of HBV transcript splicing remains poorly understood. The HBV post-transcriptional regulatory element (PRE), a highly structured *cis*-acting sequence important for facilitating the nucleocytoplasmic export of the HBV

unspliced preS/S transcript [19–21], has been implicated in the regulation of HBV pgRNA splicing [22], but the mechanism for such an effect remains elusive.

Recently, a few intronic RNA structures have been shown to promote the splicing of human *SMN2* exon 7 and *FGFR2* exon IIIb [23,24]. In order to identify the potential SREs residing in the highly structured HBV-PRE, we engineered HBV-PRE and its derivates into the intronic region of an *SMN* minigene reporter, which has been extensively studied because of its strong association with spinal muscular atrophy, a severe neurodegenerative disease [25]. We found a strong ISS residing in a 105-nucleotide element at the 3′ portion of HBV-PRE, which is distinct from previously identified elements responsible for nucleocytoplasmic export and splicing enhancement. Strikingly, the antisense strand of PRE-ISS was also fully active in repressing *SMN1* splicing, suggesting a sequence-independent regulatory mechanism. Further studies revealed that PRE-ISS folds into a double-hairpin secondary structure, with the silencing function strongly associated with this double-hairpin structure. The ISS function is also position dependent, suggesting a possible role in repressing nearby cryptic splice sites in the HBV genome. Genome-wide screening of the HBV genome predicts multiple sense–antisense (S-AS) ISSs that may fold into complex secondary structures. These results suggest an important role of structured intronic RNA elements in the regulation of pre-mRNA splicing, which may serve as a novel mechanism to repress unwanted splicing of HBV transcripts.

Results

Both the sense and antisense strands of HBV-PRE engineered in the upstream intron can repress the alternative splicing of *SMN1* exon 7

We constructed an ISS reporter in which exon 7 and the adjacent intron sequences from the *SMN1* gene were cloned into the *EGFP* coding sequence (Fig. 1A). Exon 7 of *SMN1* is dominantly included, but the potential roles of intronic cis-elements, if any, in the regulation of *SMN1* exon 7 splicing are poorly understood [23,27–31].

We tested long ($PRE_{1051–1684}$, 634 bp) and short ($PRE_{1253–1582}$, 330 bp) versions of HBV-PRE, both of which contain the essential components for splicing regulation and nucleocytoplasmic export of unspliced transcripts [20,22,32] (Fig. 1B). Both insertions resulted in significant repression of exon 7 inclusion, indicating that HBV-$PRE_{1253–1582}$ has an ISS function (Fig. 1C). The splicing repression associated with HBV-PRE does not result from the disruption of any pre-existing ISE at this intronic location, because insertion of a control sequence did not affect exon 7 inclusion (Fig. S1).

Unexpectedly, insertion of the reverse sequence of HBV-PRE (re-$PRE_{1253–1582}$, 330 bp), originally designed as a control, resulted in even stronger repression of exon 7 inclusion (Fig. 1C). This is in contrast with the reported observation that the reverse sequence did not support the pre-mRNA nuclear export activity of HBV-PRE, suggesting that different mechanisms are involved in the regulation of pre-mRNA transport and splicing. No significant sequence similarity was found between the sense and antisense strands of PRE-$HBV_{1253–1582}$ (Fig. S2A), indicating that a sequence-independent silencer function might be shared between these two different sequences. Interestingly, $PRE_{1253–1582}$ significantly

overlaps with a highly structured region in the HBV genome [21], and both the sense and antisense strands are predicted to fold into complex secondary structures (Fig. S2B).

HBV-PRE contains a 105-bp ISS element acting in both directions

To pinpoint the sequence required for the intronic silencer activity of HBV-PRE, we fragmented the full-length version of the element into four smaller pieces (PRE1–PRE4) and tested for their silencer activity. The PRE2 fragment, containing 140 bp ($PRE_{1446–1585}$), retained the full silencer activity of HBV-PRE (Fig. 1B,D). In contrast, PRE3 and PRE4 displayed no splicing silencer activity (Fig. 1D). PRE1 insertion led to aberrant splicing products (data not shown).

PRE2 was further divided into four smaller fragments, PRE2a, PRE2b, PRE2c and PRE2d, 35 bp in length each, for further mapping of the silencer sequence (Fig. 1B, bottom panel). None of the 35-bp or 70-bp fragments displayed any intronic silencer activity (Fig. 1D). Instead, PRE2bcd (105 bp, $PRE_{1481–1585}$), covering the last three-quarters of PRE2, displayed strong silencer activity comparable with the full-length PRE2 and HBV-PRE (Fig. 1D). The reverse sequence of PRE2bcd (PRE-re2bcd) also showed a similar silencer activity. None of the other combinations of PRE2 showed appreciable silencer activity. We conclude that the intronic silencer activity of HBV-PRE is confined to the nucleotide sequence from position 1481 to 1585 ($PRE_{1481–1585}$), which is referred to as PRE-ISS hereafter (Fig. 1B).

These results suggest that the newly identified 105-bp ISS from HBV-PRE affects splicing via a novel, sequence-independent mechanism. First, most sequence-specific intronic silencers are normally less than 50 bp [33–35], much shorter than PRE-ISS identified here. Second, no apparent sequence similarity was found between the sense and antisense strands of PRE-ISS, suggesting a sequence-independent silencer mechanism. Third, both the sense and antisense strands of PRE-ISS form complex secondary structures (Fig. S3), suggesting that PRE-ISS may affect splicing through its structural features.

PRE-ISS folds into a double-hairpin structure

In order to assess the possible contribution of RNA secondary structure to the silencer activity of PRE-ISS, we probed its structure by cleavage of the 5′ end labeled RNA using three ribonucleases (Fig. 2A). RNase V1 cleaves base-paired nucleotides, whereas RNase T1 and A cleave unpaired G and C/U, respectively. The results revealed that PRE-ISS forms a secondary structure consisting of two hairpins, which were named HP1 and HP2 (Fig. 2B). HP1 contains two stems (S1 and S2) and a hexanucleotide loop (L1), whereas HP2 contains a 9-bp stem (S3) and a 25-nucleotide large loop (L2). HP1 and HP2 are joined by an 11-nucleotide single-stranded region (J1/2). This secondary structure is very similar to that predicted using the RNAfold algorithm (http://rna.tbi.univie.ac.at/cgi-bin/RNAfold.cgi), except for a few details, including the absence of evidence for the predicted short base pairs inside L2 (Fig. S3B). The base pairing property of all three stems is well conserved among different HBV isolates (Fig. 2C).

All three stems of the double-hairpin structure of PRE-ISS contain significant RNase V1 signals at both strands, whereas cleavage signals by RNase T1 and RNase A are exclusively located in the unpaired loop and joint regions, including some weak signals near the bulged

U at stem S1 and the unpaired U at stem S2, which strongly supports the PRE-ISS structure shown in Fig. 2B. Interestingly, some RNase V1 signals are also observed in the unpaired regions, including one location in L1 and J1/2, and two in L2, indicating the presence of some sort of noncanonical base–base or base–backbone interaction inside these single-stranded regions. It is also noteworthy that both types of cleavage signal are present at the joint of some single-stranded and double-stranded regions, such as L1–S2 and S2–J1/2, suggesting that base pairing at these joint sites is dynamic (breathing).

In summary, RNase footprinting experiments demonstrate that PRE-ISS folds into a double-hairpin secondary structure, which is largely consistent with the computationally predicted structure. Sequence conservation analysis of PRE-ISS reveals that HP1 is less conserved than J1/2 and HP2 (Fig. 2C). Interestingly, sequence variations in three stems tend to maintain the base pairing property (Fig. 2C)./

Disruption of the double-hairpin structure abolishes the silencer activity of PRE-ISS

We next analyzed the contribution of every 15-nucleotide sequence of the first 90 nucleotides of PRE-ISS to its silencer activity. The poly-U substitution mutants were constructed, resulting in the altered sequence identity, as well as the predicted alteration of the HP1–HP2 structure in a number of cases (Fig. 3A, B).

Mutants M1, M2 and M5 displayed a silencer activity higher or comparable with that of wild-type PREISS, indicating that the silencer activity does not require specific nucleotide sequences covered in this region (Fig. 3C). M1 and M5 substitutions are located in S2 and S3, respectively, although the base pairing property of these two stems is predicted to be generally maintained (Fig. 3B). However, substitution of M2 significantly destabilizes, if not completely eliminates, S2, indicating that S2 alone is not sufficient for the silencing function of PRE-ISS. The M6 mutant, which altered the loop sequence of HP2, showed a slightly decreased silencer activity, indicating a possible function of this loop. Importantly, the M3 and M4 mutants almost completely or dramatically compromised the silencer activity (Fig. 3C). The M3 substitution is predicted to completely disrupt S1 and S2 stems and compromise the HP1 structure. M4 partially destabilizes both S1 and S3.

Collectively, the mutational analysis indicates that the silencer function of PRE-ISS is not mainly associated with any specific RNA sequences. The deleterious poly-U substitutions in M3 and M4 strongly suggest that disruption or destabilization of two of the three stems may compromise the double-hairpin structure important for silencer function. Native gel analysis of folding of the M3 and M4 mutant RNAs showed that both become less structured, as indicated by decreased gel mobility (Fig. S4). RNase footprinting experiments using the 5′ end labeled mutant RNA further demonstrated that both M3 and M4 cause the loss of at least one of their hairpins. The results in Fig. 2D reveal that the S1 and S2 regions of M3 become highly accessible to RNase T1 and A, whereas their accessibility to RNase V1 is lost, strongly suggesting that the poly-U substitution in the M3 mutant disrupts the HP1 structure as expected. The HP2 structure was substantially destabilized in the M4 mutant, and the expected loss of the terminal base pairing in S1 was also evident, indicating decreased stability of this stem (Fig. S5). We conclude from these results that the silencer activity of PRE-ISS is strongly associated with its double-hairpin structure.

Although essential, HP1 alone does not seem to be sufficient to support the silencer activity of PRE-ISS, because the PRE2bc construct harboring the complete sequence for the HP1 structure (nucleotides from position 1 to 70) showed no silencer activity (Fig. 1D). Similarly, the HP2-containing construct PREd (nucleotides 71–105) also exhibited no silencer activity (Fig. 1D). These results suggest that HP1 and HP2 collaboratively contribute to the silencer activity of PRE-ISS.

The ISS function of PRE is not mediated by PTB

The PRE-ISS element is located at the 3′ region of HBV-PRE, which overlaps with two potential PTB protein binding sites, BS1 and BS2, according to a previous report [36] (Figs 1B and 4C). Interestingly, these two sites are exclusively located in two unpaired regions of the PRE-ISS structure: J1/2 and L2, respectively (Fig. 4C). The PTB protein is well known to bind to single-stranded CU-rich sequences to mediate splicing repression [34,37]. The accessibility of PTB binding sites would provide this repressor protein with an opportunity to repress splicing. However, these binding sites are absent from the antisense strand of PRE-ISS, arguing against a potential silencer function mediated by PTB.

To directly determine the contribution of PTB binding to PRE-ISS activity, we assayed the silencer function of PRE-ISS in repressing *SMN1* exon 7 inclusion in a human hepatocellular liver carcinoma cell line HepG2-wh, which lacks the expression of the PTB protein. Figures 4A and 1D clearly show that the absence of the PTB protein did not affect the silencer activity of PRE-ISS, arguing against a role of PTB binding in this splicing repression event. To further validate the result, we performed PTB overexpression and RNAi experiments in the PTB-expressing HEK293T cell line and tested the silencer activity of PRE-ISS. Figure 4B shows that enforced or diminished PTB expression in the HEK293T cell line had little appreciable effect on PRE-ISS silencer activity.

Further evidence for PTB-independent regulation by PRE-ISS came from the analysis of the silencer activity of PRE-ISS mutants lacking PTB binding sites in the HEK293T cell line. Deletion of BS1 is not anticipated to alter the HP1–HP2 structure (Fig. 4C). This mutant showed a silencer activity comparable with wild-type PRE-ISS (Fig. 4D), supporting the conclusion that PRE-ISS does not repress alternative splicing through PTB binding to the BS1 region. Deletion of BS2 only slightly reduced the silencer activity (Fig. 4D), which is similar to that of the M6 substitution (Fig. 3C).

It is interesting to note that the M4 substitution almost completely impaired the silencer activity, but DBS1 deletion of the highly conserved nine nucleotides inside J1/2 of the 15-nucleotide poly-U substitution region of M4 had no effect. These results strongly support the conclusion that the M4 substitution compromises the silencer activity by destabilizing the S1 and S3 stems, but not by changing the sequence identity of J1/2.

PRE-ISS does not repress SP1 splicing

The ESE function of HBV-PRE has been reported previously based on its requirement for efficient splicing of the HBV pgRNA to produce the spliced SP1 product [22]. PRE-ESE resides 766 nucleotides downstream of the 3′ splice site of SP1 pgRNA (Fig. S6A). PREISS is located at the 3′ exon of the SP1 splice variant, about one kilonucleotide away from the

3′ splice site. We found that the mutant HBV pgRNA devoid of PRE-ISS (Δpre2bcd) or a large portion of it (ΔBS1 + ΔBS2) was spliced with the same efficiency as the wild-type pgRNA (Fig. S6B). We confirmed the ESE activity of HBV-PRE$_{1151–1684}$ because its deletion resulted in decreased splicing activity (Fig. S6B). The identity of the spliced SP1 RNA and the unspliced RNA with an intact 5′ splice site in our RT-PCR analysis was confirmed by sequencing analysis.

The silencer activity of the intronic PRE-ISS is position dependent

Recent studies have revealed that regulation of alternative splicing by the interaction between SREs and their interacting proteins is generally position dependent [34,38]. Considering that PRE-ISS is located in the exonic region, about 1-kb downstream of the 3′ splice site of the SP1 variant, the inability of PRE-ISS to repress SP1 splicing would not be surprising if its action is position dependent.

We therefore wished to address whether the PREISS silencer activity responds to different positions in the upstream and downstream introns (Fig. 5A). Insertion of PRE-ISS in the upstream intron 6 of the *SMN1* gene at position 1.7, 82 nucleotides from the 3′ splice site, showed the strongest silencer activity. The silencer activity decreased with increasing distance (82–182 nucleotides) from the 3′ splice site, and disappeared when the distance increased to 222 nucleotides (position 1.4) (Fig. 5B). When inserted in the downstream intron, its presence at position 1.12 (164 nucleotides) and 1.13 (224 nucleotides) displayed strong silencer activity and a reverse relationship with distance (Fig. 5B). These results suggest that the silencer activity of PRE-ISS is strongly dependent on the distance from the alternative splice site. The functional distance from the 3′ splice site is within 222 nucleotides in the upstream intron, and can extend beyond 224 nucleotides from the 5′ splice site in the downstream intron. PRE-ISS at most intronic positions showed no appreciable effect in the context of *SMN2*, in which exon 7 was almost constitutively excluded [39] (Fig. 5C).

Taken together, our results demonstrate a general silencer activity of the structure containing PRE-ISS in both the upstream and downstream introns of an alternative exon within an effective distance of about 200 nucleotides from the splice sites. The silencer activity is inversely correlated with the distance from the alternative splice sites. This position-sensitive effort explains the result that PRE-ISS does not repress SP1 splicing, because PRE-ISS is located in the distal exonic region. Indeed, PRE-ISS is located at the downstream exons of all splicing variants, with the most proximal 3′ splice site (position 1385) being about 100 nucleotides upstream. The strong silencer activity of PRE-ISS predicts the rare usage of nearby splice sites, consistent with the lack of known splicing variants of HBV transcripts in the region (Fig. 6A).

The HBV genome harbors multiple S-AS splicing silencers

HBV genes are compacted in its small genome. To maintain intact reading frames of the encoded viral proteins, the genome sequence may have evolved sophisticated mechanisms to repress aberrant splicing of the HBV pgRNA, as the unspliced pgRNA is absolutely required to produce the viral genomic DNA. In order to gain further insights into the splicing

repression mechanisms, we systematically screened potential ISSs and ESSs in the HBV genome. The genomic DNA of HBV was sliced by a cocktail of restriction enzymes. The products were then inserted into the *SMN1* and *SIRT1* splicing reporter plasmids to screen for potential ISSs and ESSs, respectively. The inserts containing ISS or ESS should result in exon skipping and an increased level of green fluorescent signal (Fig. S7A).

Ten and twelve unique ISSs and ESSs, respectively, were identified (Figs S7 and S8; Tables S1 and S2). The silencers are clustered at the 3′ regions of Pre C/Pregenome transcript (3.5 kb), pre S1 transcript (2.3 kb) and pre S2/S transcript (2.1 kb). The X transcript is enriched in both types of silencer as well, including four in the PRE region and two downstream (Fig. 6A).

Among the 10 unique ISSs, eight are S-AS pairs, whereas four of the 12 ESSs are S-AS pairs. One pair of S-AS ISSs overlaps with the first 92 nucleotides of PRE-ISS, consistent with the above conclusion that PRE-ISS acts in both orientations. It is striking that 80% of the newly identified ISSs are S-AS ISSs, suggesting that the splicing regulatory mechanism associated with the sequence-independent S-AS repression is general in maintaining intact HBV transcripts.

The alignment of genome sequences from 52 different HBV variants showed that the identified ISSs are generally located in more conserved regions in the HBV genome, whereas the ESSs have no such preference (Fig. 6B). The sequence conservation of ISSs suggests the potential importance of their primary sequences in exerting critical biological functions. Consistent with the hypothesis that the S-AS ISSs may primarily exert their splicing silencer function through their RNA secondary structures, this class of ISSs is less conserved in their primary sequence than the other ISSs, although PRE-ISS is strongly conserved (Fig. 6B).

The capability of ISSs to form stable secondary structures is generally higher than the average of the whole HBV genome sequence, although some fall below the median of the calculated minimal free energy (MFE) of the genomic background. Three pairs of S-AS, including those overlapping with PRE-ISS, have MFEs below the median, whereas the other is above (Fig. 6C). These results suggest that HBV ISSs have a large propensity to form stable secondary structures.

Discussion

Recruitment of the essential spliceosome components U1 and U2 snRNPs to the 5′ and 3′ splice sites, respectively, is the most critical step for the inclusion of an exon in the spliced mRNA. This step is highly regulated by arrays of interactions between *cis*-acting elements in pre-mRNAs and *trans*-acting splicing factors. The formation of local secondary RNA structures determines the accessibility of splice sites and *cis*-acting elements, and therefore modulates the interactions between snRNPs and splice sites, and between splicing factors and SREs, to control the splicing outcome [5,7]. An understanding of how RNA secondary structures are involved in regulated pre-mRNA splicing is central to the deciphering of the splicing code towards predicting splicing outcomes.

A splicing silencer element in HBV-PRE

HBV-PRE is a multifunctional and highly structured element located at the 3′ end of all four HBV transcripts. It contains components mediating the nucleocytoplasmic transport of the unspliced HBV PreS/S RNA, and a possible ESE that promotes the production of HBV splice variant SP1 [15]. In this study, we report that HBV-PRE also carries an ISS. This ISS is a 105-nucleotide element located at the 3′ region of HBV-PRE, distinct from the location encoding the RNA transport activity of HBV-PRE (Fig. 1B). Both the sense and antisense strands of PRE-ISS exhibit strong splicing silencer activity (Fig. 1), whereas only the sense strand of HBV-PRE displays the RNA transport function [20]. Furthermore, PRE-ISS is about 200 nucleotides downstream of the previously identified ESE in HBV-PRE [22]. Therefore, the newly identified ISS is separate from the existing elements involved in nuclear transport and ESE functions.

PRE-ISS exerts splicing silencing via RNA structure

Mutation or deletion in the human *SMN1* gene causes spinal muscular atrophy, a severe neurodegenerative disease, whereas the *SMN2* gene harboring the C → T mutation at position 6 (C6T) cannot compensate for the function of *SMN1* because this point mutation causes a shift of the major inclusion of this exon to the dominant exclusion (Fig. S1B), and therefore the production of truncated and nonfunctional survival motor neuron (SMN) protein [40,41]. Many silencer elements in the neighboring introns of *SMN* exon 7 repress exon inclusion in its *SMN2*, but not *SMN1*, splicing context [23,27,28], suggesting that the exon 7 inclusion mechanism in the *SMN1* splicing context is resistant to the effect of these ISSs. In this study, we show that PRE-ISS effectively inhibits exon 7 inclusion in the SMN1 splicing context, indicating that PRE-ISS activates an inhibitory mechanism outcompeting the exon 7 inclusion mechanism.

PRE-ISS folds into a stable double-hairpin structure *in vitro*, which is similar to that predicted by the RNAfold algorithm. Results from a systematic substitution and deletion analysis suggest that the stable double-hairpin structure is the main determinant of the silencing function of PRE-ISS, because mutations disrupting or destabilizing the double-hairpin structure, but not a single stem, strongly compromise its silencer activity (M3 and M4 shown in Fig. 3). Deletion of only one of the two PTB binding sites slightly affects the silencer activity, but depletion of PTB does not impair the silencer function of PRE-ISS. Based on these results, we propose that PRE-ISS exerts its splicing silencer function mainly via its double-hairpin structure.

This hypothesis is further supported by the fact that both the sense and antisense directions of the PRE-ISS element strongly repress exon 7 inclusion in the *SMN1* splicing context. The sense strand is highly CU rich (70.5%) and contains many single-stranded regions, whereas the antisense strand is complementarily GA rich and contains various GA-rich single-stranded regions (Fig. S3). A number of well-known silencer elements are CU rich and bound by splicing repressors to block spliceosome assembly [34,37,42,43], whereas GA-rich sequences are typical binding sites for SR proteins, a family of splicing activators that recruit spliceosome components to adjacent splice sites [44]. However, binding of SR proteins to intronic regions has been shown to repress splicing [45].

Sequence-independent enhancer activities have been reported for a pair of complementary intronic elements between exons IIIb and IIIc, two mutually exclusive exons of fibroblast growth factor receptor 2 (FGFR2), which are required for inclusion of the former exon and exclusion of the latter [24]. The base-paired structure of a 24-nucleotide ISE located close to the 5′ splice site in intron 7 of the *SMN* gene has also been shown to be critical for enhancer activity [23]. We now report that PRE-ISS represses splicing in a sequence-independent manner. Together, these findings suggest that RNA secondary structures may represent a widespread mechanism in mammals to regulate pre-mRNA splicing, either positively or negatively.

Does the intronic structured RNA represent a common mechanism for the repression of HBV genome splicing?

Splicing of the transcripts of viruses whose life cycle undergoes retrotranscription must be tightly controlled, as excessive splicing of their genomic or pgRNA would impair the integrity of their genomes and result in defective viral particles [46]. It is likely that splicing silencer elements play a crucial role in this respect, as exemplified by the well-studied HIV splicing. Here, we report that a splicing silencer may act through its secondary structure, rather than specific sequences, and that both the sense and antisense directions of the silencer show equivalent activities. Genome-wide analysis of ISS elements in the HBV genome suggests a high incidence of such ISS elements that function in both directions, representing 80% of the 10 unique ISS elements identified. This observation indicates that ISSs may have evolved as a key mechanism to prevent aberrant splicing of viral transcripts by the host splicing machinery.

Materials and methods

Constructs and mutagenesis

The pZW8-*SMN1* and pZW8-*SMN2* reporter plasmids were constructed by replacing the *SIRT* Intron5–Exon6–Intron6 alternative splicing context in pZW8 with the Intron6–Exon7–Intron7 alternative splicing context of *SMN1* and *SMN2*, respectively [26]. Full-length PRE and all PRE subelements were PCR amplified from pDM-138-PRE, a kind gift from Professor Thomas J. Hope (Northwestern University, Chicago, IL, USA), and inserted into the reporters using the engineered restriction sites *Sac*I and *Sal*I.

PRE1, 2, 3 and 4 were released from the full-length PRE1051–1684 using a mix of *Alu*I, *Dpn*I and *Hae*III. Nucleotide deletion and substitution mutations were introduced into the reporter by site-directed mutagenesis (Stratagene, La Jolla, CA, USA) using the proofreading DNA polymerase KOD plus (Toyobo, Osaka, Japan). Deletion mutants are indicated by a ‘Δ’ prefix and substitution mutants by the ‘M’ prefix. All mutations were confirmed by sequencing.

Cell culture and transfection procedure

HeLa, HEK293T, HepG2-wh (China Center for Type Culture Collection) and Huh-7 cells were grown at 37 °C with 5% CO_2 in DMEM (Invitrogen, Carlsbad, CA, USA) supplemented with 10% fetal bovine serum (Hyclone, West Logan, UT, USA). For transient

transfection assays, cells were plated 24 h prior to transfection into 24-well plates. When cells reached a confluence of 70–80%, 0.8–1 μg of plasmid was transfected into each well using Lipofectamine 2000 (Invitrogen, Carlsbad, CA, USA) following the protocol provided.

A short hairpin RNA (shRNA) hairpin DNA sequence in the pSuper-neo expression vector was expressed to knock down polypyrimidine tract binding protein (PTB) expression, and a pCDNA3.0 expression vector harboring the PTB cDNA was used to overexpress PTB. These plasmids were individually cotransfected with the indicated splicing reporter.

Western blot analysis

Cells were lysed with 1× SDS lysis buffer to prepare total cell extracts. Equal amounts of cell lysate were resolved by SDS/PAGE, followed by standard western blotting according to the manufacturer's protocol (Pall, East Hills, NY, USA).

RNA extraction and RT-PCR analysis

Cells were harvested 48 h post-transfection and total RNA was prepared using the TRIzol reagent (Invitrogen, Carlsbad, CA, USA) according to the manufacturer's protocol. Total RNA of 3 μg was incubated with random primers, dNTPs and Moloney murine leukemia virus reverse transcriptase (Promega, Madison, WI, USA) at 37 °C for 1 h to generate cDNA, followed by PCR amplification. PCR products were separated on 2% agarose gels. To assay the splicing of the reporter *SMN1* and *SMN2* minigenes, primers GFP1F (agtgcttcagccctaccc) and GFP3R (gttgtactccagcttgtgcc) were used. For the detection of the unspliced pgRNA and the SP1 splicing variant of HBV, primers SP1 (tgcccctatcctatcaacac), SP2 (actcccataggaattttccgaaa) and U2 (ttccaatgaggattaaagacag) were used.

Quantification of the splicing ratio by RT-PCR was performed using the forward primer radiolabeled with [γ–^{32}P]ATP (Furui, Beijing, China) during PCR (25 cycles in total), unless otherwise indicated. Amplicons were separated on 5% nondenaturing PAGE gels, and the spliced and unspliced RNA products were quantified by exposing the gel to phosphor screen (GE Healthcare, Milwaukee, WI, USA) and scanning with Typhoon 9200. Data were plotted using graphpad prism 4.0 and sigmaplot 11.0 programs.

Ribonuclease footprinting to determine the secondary structure of PRE-ISS

The 105-nucleotide PRE-ISS RNA was *in vitro* transcribed and gel purified followed by the 5′ end labeling reaction using [γ–^{32}P]ATP (Furui, Beijing, China) and T4 polynucleotide kinase (Fermentas, Vilnius, Lithuania). Labeled RNA samples dissolved in 10 mm Tris / HCl (pH 7.5) were heat denatured at 94 °C for 3 min, followed by rapid chilling on ice. The denatured RNA samples were then folded in buffer containing 10 mm Tris/HCl (pH 7.0), 10 mm $MgCl_2$ and 100 mm KCl at 37 °C for 5 min prior to partial cleavage by 0.05 U·μL^{-1} RNase T1 (Fermentas, China), 0.001 μg·μL^{-1} RNase A and 0.001 U·μL^{-1} RNase V1 (Ambion, Austin, TX, USA) at 37 °C for 1 min. The reactions were stopped by ribonuclease inactivation buffer following the manufacturer's protocol (Ambion, Austin, TX, USA). RNase T1 and RNase A sequencing markers were prepared following the RNase kit protocol using the RNA sequencing buffer provided, and the alkalysis marker was prepared using the alkaline hydrolysis buffer provided (Ambion, Austin, TX, USA). All samples were loaded

onto 8% sequencing gels and signals were obtained by exposing the gel to phosphor screens (GE Healthcare) and scanning with Typhoon 9200 (GE Healthcare). The collected radioactive signals were analyzed and quantified using the associated software.

Supplementary Material

Refer to Web version on PubMed Central for supplementary material.

Acknowledgements

We thank Professor Christorph Burge (Massachusetts Institute of Technology, Cambridge, MA, USA), Professor Thomas Hope (Northwestern University, Chicago, IL, USA) and Professor Tilman Heise (Medical University of South Carolina, Charleston, SC, USA) for sending us plasmids pZW8, pDM138-PRE and pCH9/3091, respectively. The authors are also indebted to members of the Yi Zhang laboratory for cooperation and discussion during the course of this investigation. This work was supported by the China 863 program (2007AA02Z112) and National Natural Science Foundation of China (30770422) to YZ, the China 973 program (2005CB724604) to YZ and XDF, the Program of Introducing Talents of Discipline to Universities (B06016) to XDF and the Program of Major Infectious Diseases such as AIDS and Viral Hepatitis Prevention and Control (2008ZX10001-002) to YZ.

Abbreviations

ESE	exonic splicing enhancer
ESS	exonic splicing silencer
FGFR2	fibroblast growth factor receptor 2
HBV	hepatitis B virus
ISE	intronic splicing enhancer
ISS	intronic splicing silencer
MFE	minimal free energy
pgRNA	pre-genomic RNA
PRE	post-transcriptional regulatory element
PTB	polypyrimidine tract binding protein
S-AS	sense–antisense
shRNA	short hairpin RNA
SMN	survival motor neuron
SRE	splicing regulatory element

References

1. Wang ET & Sandberg R (2008) Alternative isoform regulation in human tissue transcriptomes. Nature 456, 470–476. [PubMed: 18978772]
2. Pan Q, Shai O, Lee FJ, Frey BJ & Blencowe BJ (2008) Deep surveying of alternative splicing complexity in the human transcriptome by high-throughput sequencing. Nat Genet 40, 1413–1415. [PubMed: 18978789]

3. Cooper TA (2005) Alternative splicing regulation impacts heart development. Cell 120, 1–2. [PubMed: 15652472]
4. Li Q, Lee JA & Black DL (2007) Neuronal regulation of alternative pre-mRNA splicing. Nat Rev Neurosci 8, 819–831. [PubMed: 17895907]
5. Wang Z & Burge CB (2008) Splicing regulation: from a parts list of regulatory elements to an integrated splicing code. RNA 14, 802–813. [PubMed: 18369186]
6. Black DL (2003) Mechanisms of alternative pre-messenger RNA splicing. Annu Rev Biochem 72, 291–336. [PubMed: 12626338]
7. Hertel KJ (2008) Combinatorial control of exon recognition. J Biol Chem 283, 1211–1215. [PubMed: 18024426]
8. Shepard PJ & Hertel KJ (2008) Conserved RNA secondary structures promote alternative splicing. RNA 14, 1463–1469. [PubMed: 18579871]
9. Warf MB & Berglund JA (2010) Role of RNA structure in regulating pre-mRNA splicing. Trends Biochem Sci 35, 169–178. [PubMed: 19959365]
10. Buratti E & Baralle FE (2004) Influence of RNA secondary structure on the pre-mRNA splicing process. Mol Cell Biol 24, 10505–10514. [PubMed: 15572659]
11. Buratti E, Muro AF, Giombi M, Gherbassi D, Laconcig A & Baralle FE (2004) RNA folding affects the recruitment of SR proteins by mouse and human polypurinic enhancer elements in the fibronectin EDA exon. Mol Cell Biol 24, 1387–1400. [PubMed: 14729981]
12. Giedroc DP & Cornish PV (2009) Frameshifting RNA pseudoknots: structure and mechanism. Virus Res 139, 193–208. [PubMed: 18621088]
13. Balvay L, Soto RR, Ricci EP, Decimo D & Ohlmann T (2009) Structural and functional diversity of viral IRESes. Biochim Biophys Acta 1789, 542–557. [PubMed: 19632368]
14. Saliou JM, Bourgeois CF, Ayadi-Ben ML, Ropers D, Jacquenet S, Marchand V, Stevenin J & Branlant C (2009) Role of RNA structure and protein factors in the control of HIV-1 splicing. Front Biosci 14, 2714–2729.
15. Sommer G & Heise T (2008) Posttranscriptional control of HBV gene expression. Front Biosci 13, 5533–5547. [PubMed: 18508603]
16. Park GS, Kim HY, Shin HS, Park S, Shin HJ & Kim K (2008) Modulation of hepatitis B virus replication by expression of polymerase-surface fusion protein through splicing: implications for viral persistence. Virus Res 136, 166–174. [PubMed: 18562032]
17. Ma ZM, Lin X, Wang YX, Tian XC, Xie YH & Wen YM (2009) A double-spliced defective hepatitis B virus genome derived from hepatocellular carcinoma tissue enhanced replication of full-length virus. J Med Virol 81, 230–237. [PubMed: 19107969]
18. Soussan P, Tuveri R, Nalpas B, Garreau F, Zavala F, Masson A, Pol S, Brechot C & Kremsdorf D (2003) The expression of hepatitis B spliced protein (HBSP) encoded by a spliced hepatitis B virus RNA is associated with viral replication and liver fibrosis. J Hepatol 38, 343–348. [PubMed: 12586301]
19. Huang J & Liang TJ (1993) A novel hepatitis B virus (HBV) genetic element with Rev response element-like properties that is essential for expression of HBV gene products. Mol Cell Biol 13, 7476–7486. [PubMed: 8246965]
20. Donello JE, Beeche AA, Smith GJ III, Lucero GR & Hope TJ (1996) The hepatitis B virus posttranscriptional regulatory element is composed of two subelements. J Virol 70, 4345–4351. [PubMed: 8676457]
21. Patzel V & Sczakiel G (1997) The hepatitis B virus posttranscriptional regulatory element contains a highly stable RNA secondary structure. Biochem Biophys Res Commun 231, 864–867. [PubMed: 9070912]
22. Heise T, Sommer G, Reumann K, Meyer I, Will H & Schaal H (2006) The hepatitis B virus PRE contains a splicing regulatory element. Nucleic Acids Res 34, 353–363. [PubMed: 16410615]
23. Miyaso H, Okumura M, Kondo S, Higashide S, Miyajima H & Imaizumi K (2003) An intronic splicing enhancer element in survival motor neuron (SMN) pre-mRNA. J Biol Chem 278, 15825–15831. [PubMed: 12604607]

24. Muh SJ, Hovhannisyan RH & Carstens RP (2002) A non-sequence-specific double-stranded RNA structural element regulates splicing of two mutually exclusive exons of fibroblast growth factor receptor 2 (FGFR2). J Biol Chem 277, 50143–50154. [PubMed: 12393912]
25. Singh RN (2007) Evolving concepts on human SMN pre-mRNA splicing. RNA Biol 4, 7–10. [PubMed: 17592254]
26. Liu W, Zhou Y, Hu Z, Sun T, Denise A, Fu XD & Zhang Y (2010) Regulation of splicing enhancer activities by RNA secondary structures. FEBS Lett 584, 4401–4407. [PubMed: 20888818]
27. Singh NK, Singh NN, Androphy EJ & Singh RN (2006) Splicing of a critical exon of human survival motor neuron is regulated by a unique silencer element located in the last intron. Mol Cell Biol 26, 1333–1346. [PubMed: 16449646]
28. Miyajima H, Miyaso H, Okumura M, Kurisu J & Imaizumi K (2002) Identification of a cis-acting element for the regulation of SMN exon 7 splicing. J Biol Chem 277, 23271–23277. [PubMed: 11956196]
29. Singh NN, Singh RN & Androphy EJ (2007) Modulating role of RNA structure in alternative splicing of a critical exon in the spinal muscular atrophy genes. Nucleic Acids Res 35, 371–389. [PubMed: 17170000]
30. Kashima T, Rao N & Manley JL (2007) An intronic element contributes to splicing repression in spinal muscular atrophy. Proc Natl Acad Sci USA 104, 3426–3431. [PubMed: 17307868]
31. Gladman JT & Chandler DS (2009) Intron 7 conserved sequence elements regulate the splicing of the SMN genes. Hum Genet 126, 833–841. [PubMed: 19701774]
32. Smith GJ III, Donello JE, Luck R, Steger R & Hope TJ (1998) The hepatitis B virus post-transcriptional regulatory element contains two conserved RNA stem-loops which are required for function. Nucleic Acids Res 26, 4818–4827. [PubMed: 9776740]
33. Carstens RP, Wagner EJ & Garcia-Blanco MA (2000) An intronic splicing silencer causes skipping of the IIIb exon of fibroblast growth factor receptor 2 through involvement of polypyrimidine tract binding protein. Mol Cell Biol 20, 7388–7400. [PubMed: 10982855]
34. Xue Y, Zhou Y, Wu T, Zhu T, Ji X, Kwon YS, Zhang C, Yeo G, Black DL, Sun H et al. (2009) Genome-wide analysis of PTB–RNA interactions reveals a strategy used by the general splicing repressor to modulate exon inclusion or skipping. Mol Cell 36, 996–1006. [PubMed: 20064465]
35. Sen S, Talukdar I & Webster NJ (2009) SRp20 and CUG-BP1 modulate insulin receptor exon 11 alternative splicing. Mol Cell Biol 29, 871–880. [PubMed: 19047369]
36. Zang WQ, Li B, Huang PY, Lai MM & Yen SS (2001) Role of polypyrimidine tract binding protein in the function of the hepatitis B virus posttranscriptional regulatory element. J Virol 75, 10779–10786. [PubMed: 11602719]
37. Sawicka K, Bushell M, Spriggs KA & Willis AE (2008) Polypyrimidine-tract-binding protein: a multifunctional RNA-binding protein. Biochem Soc Trans 36, 641–647. [PubMed: 18631133]
38. Corrionero A & Valcarcel J (2009) RNA processing: redrawing the map of charted territory. Mol Cell 36, 918–919. [PubMed: 20064456]
39. Horne C & Young PJ (2009) Is RNA manipulation a viable therapy for spinal muscular atrophy? J Neurol Sci 287, 27–31. [PubMed: 19758605]
40. Lorson CL, Hahnen E, Androphy EJ & Wirth B (1999) A single nucleotide in the SMN gene regulates splicing and is responsible for spinal muscular atrophy. Proc Natl Acad Sci USA 96, 6307–6311. [PubMed: 10339583]
41. Burghes AH & Beattie CE (2009) Spinal muscular atrophy: why do low levels of survival motor neuron protein make motor neurons sick? Nat Rev Neurosci 10, 597–609. [PubMed: 19584893]
42. Shukla S, Del Gatto-Konczak F, Breathnach R & Fisher SA (2005) Competition of PTB with TIA proteins for binding to a U-rich cis-element determines tissue-specific splicing of the myosin phosphatase targeting subunit 1. RNA 11, 1725–1736. [PubMed: 16177139]
43. Sharma S, Kohlstaedt LA, Damianov A, Rio DC & Black DL (2008) Polypyrimidine tract binding protein controls the transition from exon definition to an intron defined spliceosome. Nat Struct Mol Biol 15, 183–191. [PubMed: 18193060]
44. Wang J, Smith PJ, Krainer AR & Zhang MQ (2005) Distribution of SR protein exonic splicing enhancer motifs in human protein-coding genes. Nucleic Acids Res 33, 5053–5062. [PubMed: 16147989]

45. Ibrahim EC, Schaal TD, Hertel KJ, Reed R & Maniatis T (2005) Serine/arginine-rich protein-dependent suppression of exon skipping by exonic splicing enhancers. Proc Natl Acad Sci USA 102, 5002–5007. [PubMed: 15753297]

46. Stoltzfus CM & Madsen JM (2006) Role of viral splicing elements and cellular RNA binding proteins in regulation of HIV-1 alternative RNA splicing. Curr HIV Res 4, 43–55. [PubMed: 16454710]

47. Crooks GE, Hon G, Chandonia JM & Brenner SE (2004) WebLogo: a sequence logo generator. Genome Res 14, 1188–1190. [PubMed: 15173120]

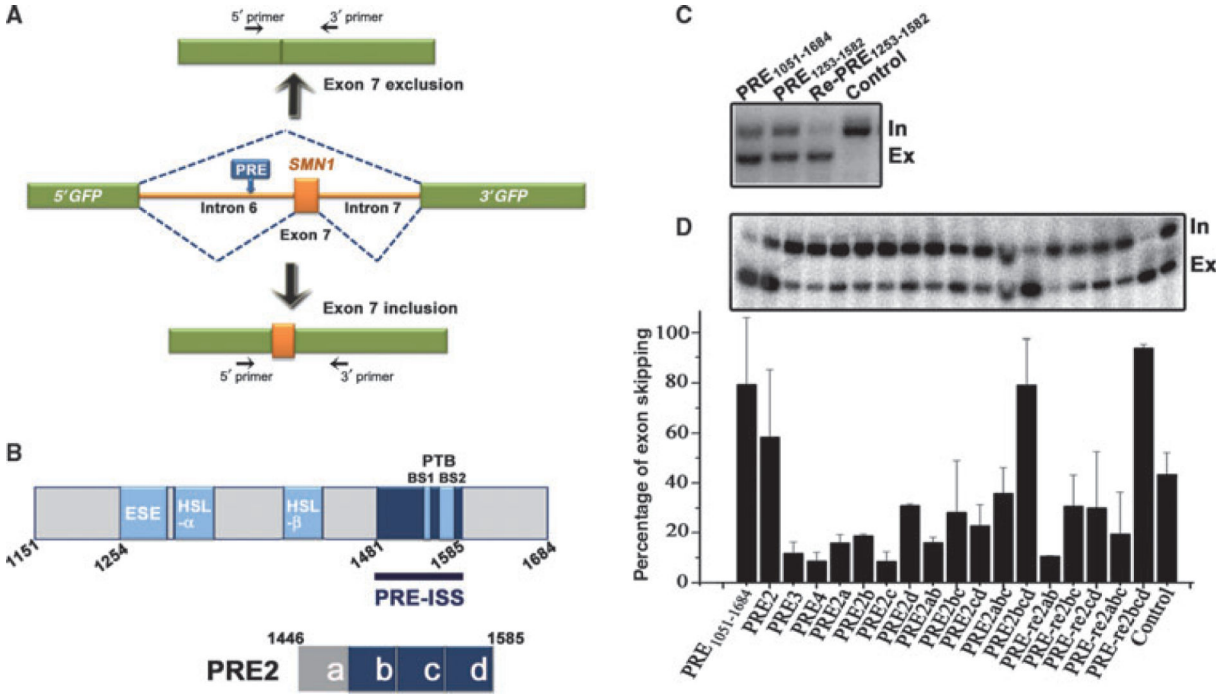

Fig. 1.

(A) Schematic representation of the reporter plasmid pZW8-*SMN1*. The EGFP gene (green) was split into the 5′ and 3′ parts by the *SMN1* alternative splicing cassette (orange) including exon 7 and parts of the upstream intron 6 and downstream intron 7. HBV-PRE and its derivatives were cloned into intron 6 at the location 122 bp upstream of the 3′ splice site of exon 7 in the reporter plasmid pZW8-SMN1C (1.6). The positions of the 5′ and 3′ primers used to amplify the splicing products are indicated by arrows. (B) Schematic drawing of the position of the functional elements (boxed in light blue) residing in the HBV post-transcriptional regulatory element (PRE) [15]. The intronic splicing silencer (PRE-ISS) (in dark blue) identified in this study is also indicated. (C) ISS function of the long and short versions of HBV-PRE, $PRE_{1051–1684}$, $PRE_{1253–1582}$ (sense direction) and $Re\text{-}PRE_{1253–1582}$ (antisense direction), in HeLa cells. ‘Control’ indicates the *SMN1* reporter plasmid without any insertion. The band ‘In’ indicates the splicing product with exon 7 inclusion, and ‘Ex’ indicates the exon exclusion product. (D) [γ–^{32}P]-Labeled RT-PCR products of the splicing products in HepG2-wh cells from the *SMN1* reporter plasmids containing different fragments from $HBV\text{-}PRE_{1051–1684}$ shown below the graphic representation (bottom panel). A representative gel is shown in the top panel, and the graph below shows the percentage of exon exclusion, indicating the percentage of the splicing product with exon 7 exclusion (‘Ex’ band) among the total products (a sum of ‘Ex’ and ‘In’ bands) from three independent experiments, with the standard deviation (SD) being shown.

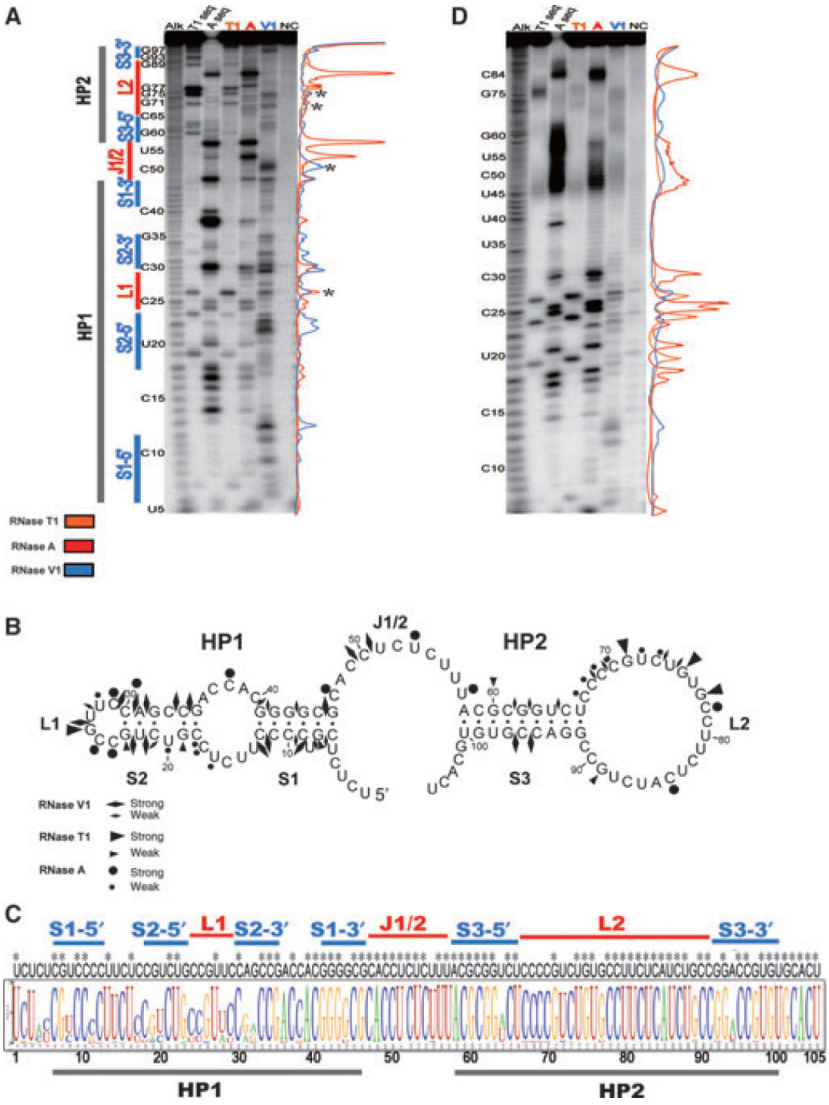

Fig. 2.

RNase footprinting analysis of the secondary structure of PRE-ISS. (A) RNase footprinting analysis of the fragments of the 5′ end labeled and folded PRE-ISS wild-type RNA, which was cleaved by RNase T1, RNase V1 and RNase A. The T1 seq and A seq lanes represent RNase T1 and RNase A sequencing markers, respectively. NC indicates the negative control RNA sample produced by adding water instead of an RNase. Colored curves represent the normalized intensity of RNase cleavage signals, and asterisks indicate RNase V1 signals in unpaired regions. (B) Deduced secondary structure of the PRE-ISS RNA. RNase T1, RNase V1 and RNase A signals are superimposed on the secondary structure. Triangles, diamonds and ellipses represent signals for RNase T1, RNase V1 and RNase A, respectively; larger ones represent stronger signals and smaller ones weaker signals. (C) Conservation analysis of the PRE-ISS sequence. The conservation in 52 HBV genomes was calculated and the graphic representation was created by WebLogo 3 [47]. The HP1 and HP2 regions are indicated, with stems being marked by cyan bars and the RNase-accessible joint and loop

regions by red bars. (D) RNase footprinting analysis of products from the ribonuclease cleavage of the M3 mutant RNA of PRE-ISS.

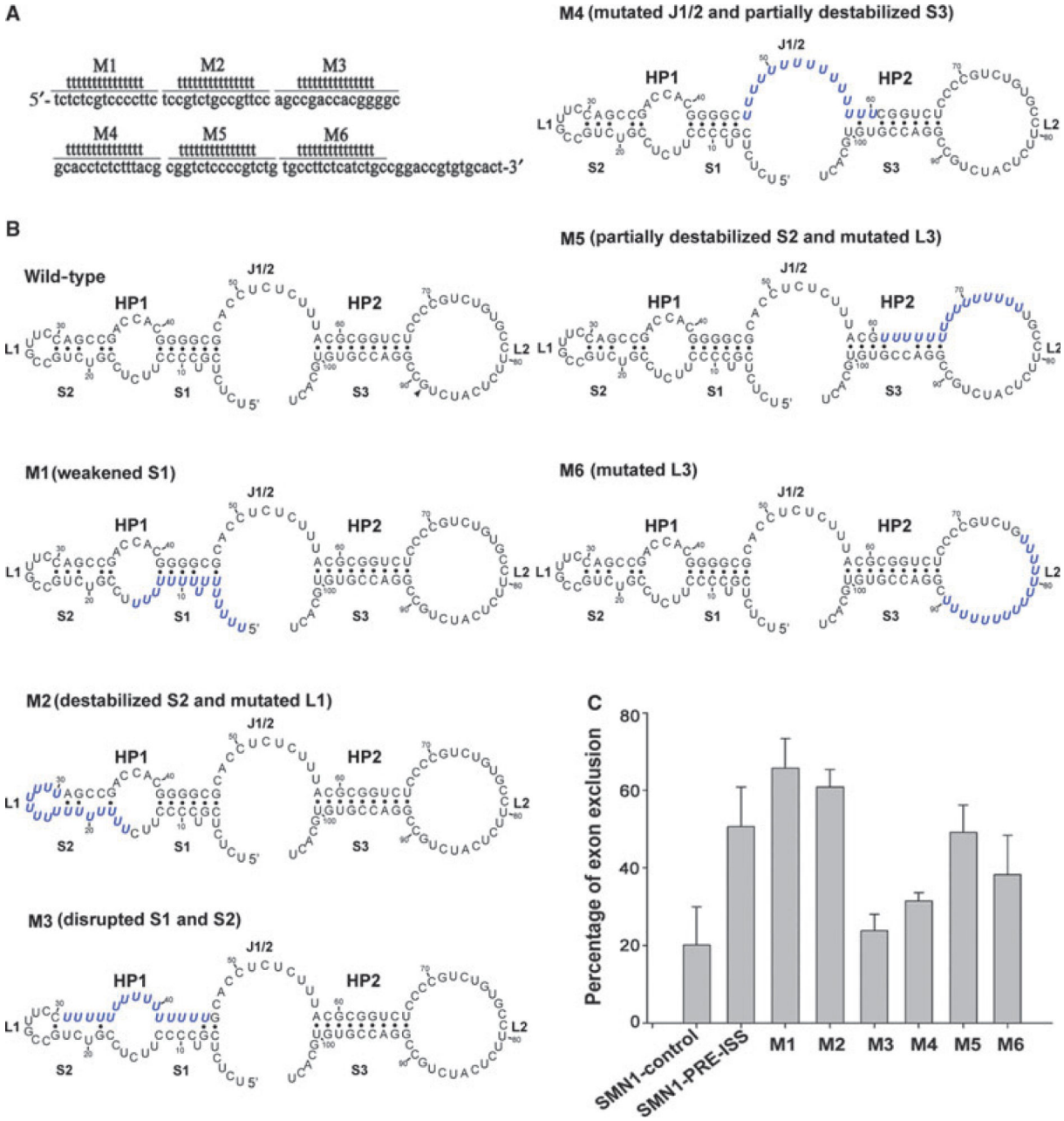

Fig. 3.

Poly-U substitution analysis of the relationship between the sequence/structure and silencer function of PRE-ISS. (A) Schematic representation of the 15T substitution mutants of PRE-ISS inserted in the reporter plasmid pZW8-SMN1C (1.6) (see Fig. 1), with the substitution position of each mutant being indicated. (B) The predicted effect of each poly-U substitution on the HP1–HP2 structure. (C) Quantification of the splicing silencer activity (percentage of exon exclusion) of each poly-U substitution mutant of PRE-ISS in HEK293T cells. *SMN1* control is the empty *SMN1* reporter plasmid. The experiments and quantification of the percentage of exon exclusion were similar to those in Fig. 1C, D.

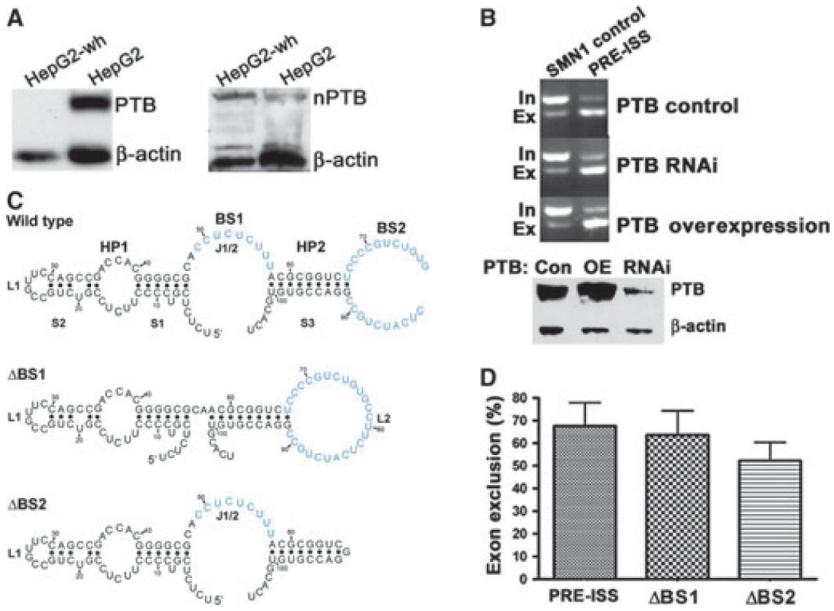

Fig. 4.

PRE-ISS regulation is independent of PTB expression. (A) Western blot analysis of the PTB and nPTB protein level in HepG2-wh cells, with b-actin as a loading control. (B) PTB RNAi and overexpression in HEK293T cells. RNAi and overexpression of PTB were carried out using a PTB1-specific shRNA and a PTB1 cDNA expressed from pSuper-neo and pcDNA3, respectively [34]. PTB protein levels in treated and control cells were analyzed by western blot (bottom). In treated and control cells, *SMN1* control plasmid or the plasmid containing PRE-ISS inserted into the reporter plasmid pZW8-SMN1C (1.12) were transfected, and the silencer function of PRE-ISS was analyzed by RT-PCR (top panels). The position of 1.12 is in intron 7 (see Figs 4A and S1). (C) Schematic diagram of the predicted effect of the deletion of either of the two PTB binding sites (BS1 and BS2) on the structure of PRE-ISS. (D) Quantification of the splicing silencer activity of PTB-ISS and two deletion mutants (C) in HEK293T cells, similar to that in Fig. 1C, D.

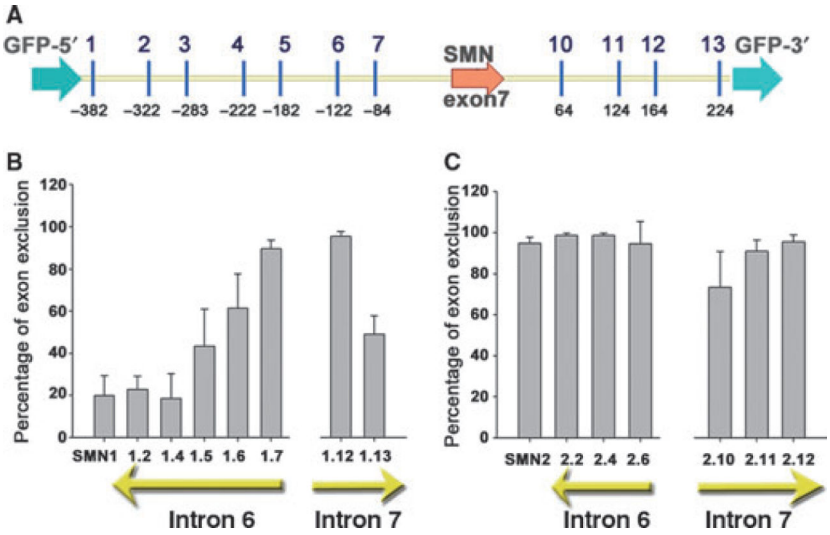

Fig. 5.

The positional effect of the PRE-ISS silencing activity. (A) Schematic illustration of the insertion at different positions. Numbers 1, 2, 3, 4, 5, 6 and 7 represent locations 382, 322, 283, 222, 182, 122 and 84 nucleotides upstream of the 3′ splice site of exon 7, respectively, whereas numbers 10, 11, 12 and 13 represent locations 64, 124, 164 and 224 nucleotides downstream of the 5′ splice site of exon 7, respectively. All the constructs in the *SMN1* exon 7 background are named as 1.1, 1.2, etc.; all constructs in the *SMN2* context are named as 2.1, 2.2, etc. (B) Radioactive RT-PCR to analyze the silencer effect of PRE-ISS inserted into different locations in the *SMN1* reporter plasmid. Lane *SMN1* indicates the empty *SMN1* reporter plasmid transfected in HEK293T cells. (C) The silencer effect of PRE-ISS inserted into different locations in the *SMN2* reporter plasmid.

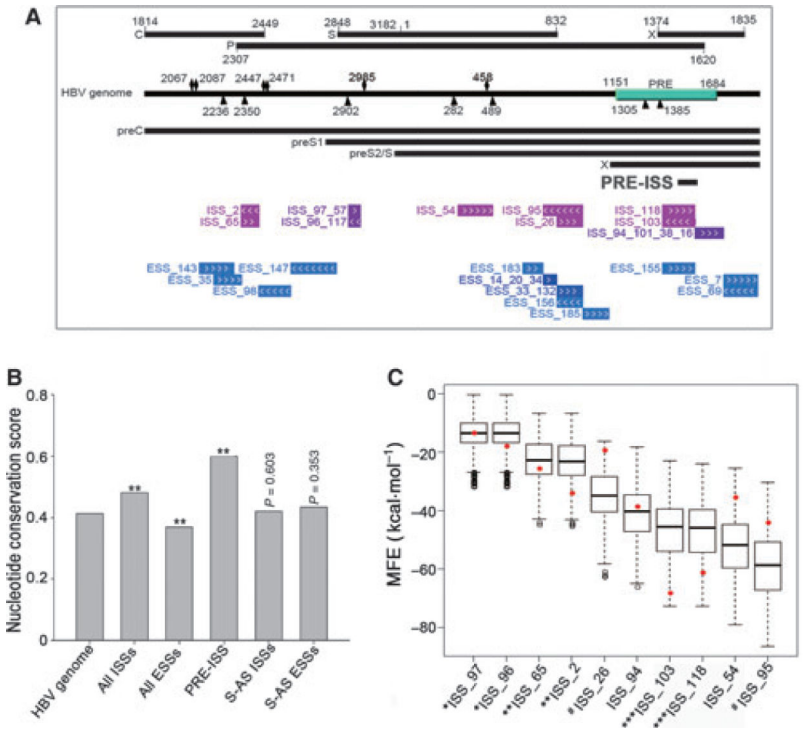

Fig. 6.

(A) Mapping of potential ESS and ISS elements in the HBV genome that enhanced splicing of the alternative *SIRT1* exon (ESSs) or repressed splicing of the alternative *SMN1* exon (ISSs) in HeLa cells (see Data S1 for details). ESSs are depicted in blue and ISSs in purple, with their corresponding plasmid clones indicated on the left. ESSs and ISSs recovered at higher frequencies are presented in darker colors. Arrowheads to the right and to the left in ESS and ISS boxes represent sense and antisense sequences, respectively. The HBV genome is delineated with the known 5′ and 3′ splice sites indicated by diamonds and triangles, respectively. The location of the PRE element on the HBV genome is boxed in green. The four translational products are shown above the genome, whereas the four transcripts are shown below. PRE-ISS is shown below the transcripts and above the selected ISSs. (B) Nucleotide conservation scores of the HBV genome and different groups of ESSs and ISSs. The score was obtained by analyzing 52 HBV genomes on the RNAz webserver (http://rna.tbi.univie.ac.at/cgi-bin/RNAz.cgi). The double asterisk indicates $P < 0.001$ in a t-test between the HBV genome and different splicing element groups (see Materials and methods). (C) Minimal free energy (MFE) values of the predicted secondary structures of candidate ISSs and their background sequences from the HBV genome, which were calculated by the RNAfold program. The dots (red) represent MFE values of the indicated ISSs. The genome background MFEs of a specific ISS were obtained by customized sliding windows in the HBV genome, resulting in a total of 3182 background sequences for each ISS. The box plot of MFEs of all background sequences for a specific ISS was obtained using R (http://www.r-project.org). The broken line and box (black) represent the distribution of MFE values of the HBV genome background against each ISS. The bold line in the box represents the median of the MFE values. The box covers 50% of the MFE

values. The broken lines indicate MFEs inside the normal distribution, whereas the outliers stand for the MFEs beyond.